Toward Image-Based Facial Hair Modeling

Tomas Lay Herrera
University of Bonn

Arno Zinke
GfaR GmbH

Andreas Weber[*]
University of Bonn

Thomas Vetter[†]
University of Basel

Abstract

In this paper we present a novel efficient and fully automated technique to synthesize realistic facial hair—such as beards and eyebrows—on 3D head models. The method requires registered texture images of a target model on which hair needs to be generated. In a first stage of our two-step approach a statistical measure for hair density is computed for each pixel of the texture. In addition, other geometric features such as 2D pixel orientations are extracted, which are subsequently used to generate a 3D model of the individual hair strands. Missing or incomplete information is estimated based on statistical models derived from a database of texture images of over 70 individuals. Using the new approach, characteristics of the hair extracted from a given head may be also transferred to another target.

1 Introduction

The modeling of plausible hairstyles is an essential aspect in the creation of believable virtual characters, as they improve realism considerably. Nevertheless, the large number of hair strands in combination with their inherent complexity (thin and long structures that interact freely with each other) make this task one of the most challenging in this field. Current approaches on hair modeling are based on interactive techniques [Ward et al. 2007; Mihashi et al. 2005] that require a high grade of expertise of the user, or rely on information obtained from multiple viewpoints [Paris et al. 2008; Wei et al. 2005]. Although the latter approach is more automated, it is very time consuming and resource demanding.

On the other hand, techniques for hair detection on images have already been presented. However, they either rely on color information [Yacoob and Davis 2006] or combine the color information with the frequency one in a rather simplistic way [Rousset and Coulon 2008].

In contrast to scalp hair, the appearance of facial hair—which is important for realism as well—is much more constrained and the lengths of the filaments tend to be considerably shorter. Even though their characteristics are quite different from scalp hair, no other dedicated techniques taking advantage of such specific properties have been presented in literature.

As will be shown in this work, plausible facial hair such as short beards and eyebrows can be generated very efficiently taking a fully automated approach. Our main contribution is the implementation of a novel technique that takes as input a 3D head model (source model S) with its texture images [Blanz and Vetter 1999; Paysan et al. 2009] and which generates plausible facial hair strands with minimum user interaction. In detail, our approach includes the following key features:

---

[*]e-mail: {tomas,zinke,weber}@cs.uni-bonn.de
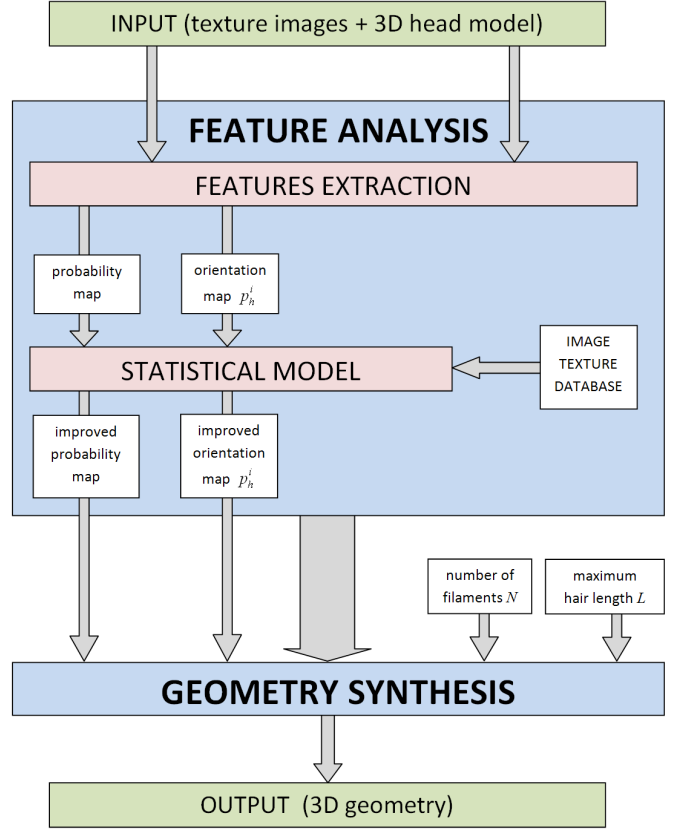[†]e-mail: Thomas.Vetter@unibas.ch

Figure 1: Workflow of the whole process

- A novel measure estimating the probability of a pixel to belong to either skin or hair which is inferred from statistics of the texture image of a source model S. The new approach works fully automated and is robust with respect to color tone variations of both skin and hair.

- A method for estimating 2D strand orientation as well as hair density in texture space.

- A statistical prior based on features of over 70 individuals that improves the plausibility of results even in difficult cases with missing or incomplete texture information.

- A particle shooting method that eventually generates a fiber based 3D hair model.

- Using the new approach characteristics of the hair extracted from a given source S can be transferred to other head (target model T).

2 Overview

Our approach has basically two-stages, cf. Figure 1: in the "feature analysis" step we use image processing techniques to calculate pixel-wise features on the texture image of S that help us to estimate the distribution of hair, together with the corresponding 2D orientation. Furthermore, by applying the "feature extraction" to a database of many individuals (which is a pre-processing step), we estimate a statistical prior representing the a-priory likelihood of hair distribution embedded in the database. This prior information is used to improve results of synthesizing facial hair in case of missing or incomplete source data.

The "geometry synthesis" step involves the conversion of the 2D features to 3D. This step relies on the fact that the texture images are registered at the 3D head models. The resulting facial hair geometry is then rendered using the framework proposed in [Zinke and Weber 2007] in order to achieve photo-realistic results.

3 Feature Analysis

The first and most challenging task of the "Feature Analysis" step is to identify regions in the texture image of S where hair is present. This identified region and the 2D texture orientation (cf. Section 3.3) enable us to characterize the facial hair of source. Subsequently, as described in section 4, we synthesize hair on T. This facial hair transfer is possible because all texture images are assumed to be registered and thus a fixed one-to-one correspondence between texels of S and T exists.

For our estimation purposes, we distinguish two regions: a hair region and a skin region, where every pixel in the image belongs either to the former or to the latter. Following this idealized consideration, the probability of a texel $t_{(i,j)}$, $p_{\text{hair}}^{(i,j)}$, for belonging to hair is estimated. The resulting map is characterizing the facial hair distribution that we are looking for.

3.1 A Feature Set for Discriminating Skin and Hair

Purely color-based techniques, widely used in skin detection, are not accurate in case of shadowing and highlights as such features tend to have a drastic effect on the tonality of a texel, cf. [Kakumanu et al. 2007]. Moreover, the coloring of both hair and skin may be rather similar making a purely color-based discrimination problematic. To improve the stability of results not only color but also geometric features have been used for classification.

Our full feature vector as illustrated in Figure 2 includes the following components:

- The "strength of orientation" o, response of the orientation filter along the dominant angle (cf. Equation 10). Hair regions tend to have a predominant growth direction.

- The absolute value of the local texture gradient g helps to discriminate between rather smooth ("low frequency") skin and less homogeneous ("high frequency") hair regions.

- The Luminance L—as the sum of the red, green and blue color channels—is used to characterize the brightness (as energy) of a texel.

- $R - G$ and $R - B$ represent the difference of the red channel with the green and with the blue one, respectively. Besides relating green and blue to the strength of the red component (dominating skin color due to blood flow in the dermis independent of complexion) these differences also reduce the effect of specular skin highlights.
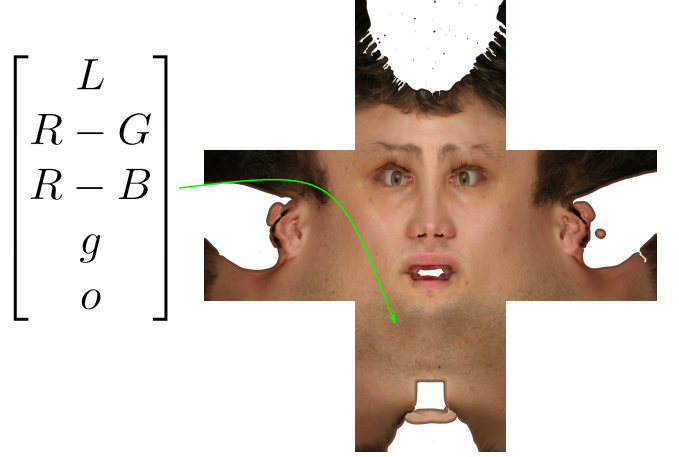

Figure 2: The feature set is computed on a per pixel basis.

3.2 An Iterative Approach for Estimating the Distribution of Facial Hair

Based on the feature set introduced above the probabilities $p_{\text{hair}}^{(i,j)}$ is computed. For that purpose we take a novel fully automated statistical approach. Assuming that the typical characteristics of both skin and hair can be sufficiently well characterized by small exemplary "learning regions" in the texture of S we iteratively proceed as follows.

First, two square texture blocks—one for skin and another for hair—are randomly selected. For each of the two regions we generate a group of histograms, one per feature, using the information stored on the pixel-wise calculated feature vectors (see Figure 3). Subsequently a naive Bayesian estimator is used to calculate $p_{\text{hair}}^{(i,j)}$. In each iteration also a measure estimating the quality of the classification is computed. Eventually, after a user-defined number of iterations, the best result with respect to this measure is kept. In the following, the approach will be discussed in more detail.

3.2.1 Computing $p_{\text{hair}}^{(i,j)}$

Let $\widetilde{H}$ and $\widetilde{S}$ denote selected learning regions for skin and hair and $\left|\widetilde{H}\right|$ and $\left|\widetilde{S}\right|$ their corresponding cardinalities.

Initially, a first estimate $\mu_{\text{hair}}^{(i,j)}$ ($\mu_{\text{skin}}^{(i,j)}$) for the probability of a texel $t_{(i,j)}$ for belonging to hair (skin) region is computed, according to our feature set $X = \{x_k\}$, with k indexed over the features $\{L, R - G, R - B, g, o\}$. These estimators will

be used in a subsequent step to calculate the final probability values(cf. Equation 6).

Directly dealing with high dimensional feature vectors $X^{(i,j)}$ is not practical as this would require orders of magnitude more feature space samples (than provided by the two skin and hair learning regions) to obtain meaningful statistical results. For that reason all statistics are first computed independently for each of its components $x_k^{(i,j)}$ taking a naive Bayesian estimation approach and are then combined to finally obtain the posterior probability $p_{\text{hair}}^{(i,j)}$.

Suppressing the (i,j)-dependence and using Bayes formula the following holds:

$$\mu_{\text{hair}}^k = P(\text{hair} \mid x_k = h_k^n) = \frac{P(\text{hair} \cap x_k = h_k^n)}{P(x_k = h_k^n)} \quad (1)$$

where h_k^n is denoting the n-th bin in the corresponding x_k-histogram h_k.

Substituting with $\left|\widetilde{H}\right|$ and $\left|\widetilde{S}\right|$ yields

$$\mu_{\text{hair}}^k = \frac{\frac{\left|\widetilde{H}_{(x_k=h_k^n)}\right|}{|\widetilde{H} \cup \widetilde{S}|}}{\frac{\left|\widetilde{H}_{(x_k=h_k^n)} \cup \widetilde{S}_{(x_k=h_k^n)}\right|}{|\widetilde{H} \cup \widetilde{S}|}} \quad (2)$$

and after eliminating denominators we arrive at

$$\mu_{\text{hair}}^k = \frac{\left|\widetilde{H}_{(x_k=h_k^n)}\right|}{\left|\widetilde{H}_{(x_k=h_k^n)} \cup \widetilde{S}_{(x_k=h_k^n)}\right|}. \quad (3)$$

The probability estimates μ_{skin}^k are then combined by the following weighted average heuristic taking into account the spread of the histograms h_k:

$$\frac{1}{\sigma_{\text{hair}}^2} = \sum_k \frac{1}{\sigma_k^2} \quad (4)$$

$$\mu_{\text{hair}} = \frac{1}{\sigma_{\text{hair}}^2} \sum_k \frac{\mu_{\text{hair}}^k}{\sigma_k^2}. \quad (5)$$

Here, σ_k is denoting the normalized standard deviations[1] of the histograms h_k.

Although this simplistic approach is optimal for combining Gaussian probability densities only, it works surprisingly well in our case.

An expression for μ_{skin}^k can be derived similarly.

The results of applying (5) $\mu_{\text{hair}}^{(i,j)}$ and $\mu_{\text{skin}}^{(i,j)}$ contain complementary information about the distribution of facial hair. Ideally, the two values should sum up to one, for each texel $t_{(i,j)}$. Considering this property the probability estimates can be improved further by combining $\mu_{\text{hair}}^{(i,j)}$ and $\mu_{\text{skin}}^{(i,j)}$ according to:

$$p_{\text{hair}}^{(i,j)} = \sqrt{\mu_{\text{hair}}^{(i,j)} \cdot (1 - \mu_{\text{skin}}^{(i,j)})} \quad (6)$$

---

[1]The standard deviations are normalized by the range of feature values present in the texture of the source S.
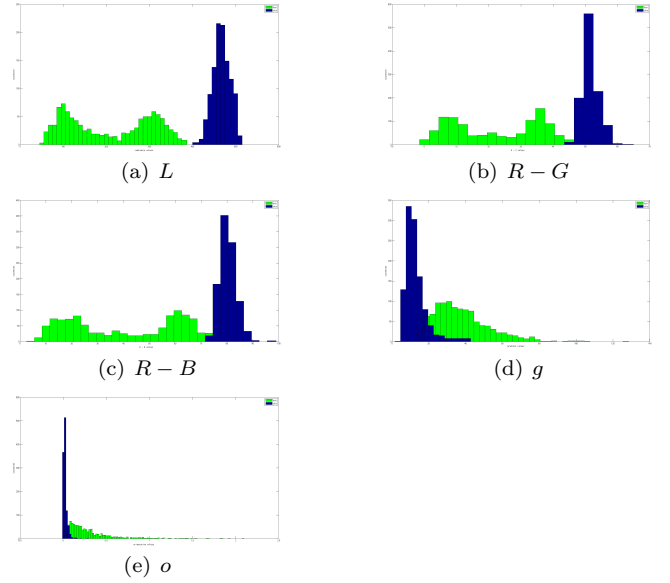

(a) L

(b) $R - G$

(c) $R - B$

(d) g

(e) o

Figure 3: Typical histograms h_k for each of the feature set components x_k derived from the selected hair(green) and skin(blue) regions. Please note their difference in distribution.

$$p_{\text{skin}}^{(i,j)} = \sqrt{\mu_{\text{skin}}^{(i,j)} \cdot (1 - \mu_{\text{hair}}^{(i,j)})}. \quad (7)$$

As will be discussed in the following sections the probabilities $p_{\text{hair}}^{(i,j)}$ are used to characterize the distribution of facial hair.

3.2.2 A Quality Measure for Classification

In each iteration $k \in \{1, .., n\}$ of the proposed method hair and skin learning regions are selected and the probabilities $p_{\text{hair}}^{(i,j)}$ are computed. The selection is completely random, we just ensure that each selected region lies completely over the texture image. The region with the lowest gradient g (averaged over all the pixels) is declared as "skin". To identify optimal results a simple but efficient heuristic is used.

Assuming that a selection is suitable if a clear classification (as either hair or skin) is possible, the quality measure m^k is computed as follows:

$$m^k = \sum_{i,j} \max(p_{\text{skin}}^{(i,j)}, p_{\text{hair}}^{(i,j)}). \quad (8)$$

The optimum of m_{best} is given for the iteration (i.e. the pair of regions) that maximizes the separation of assumed skin and hair texels:

$$m_{\text{best}} = \max(m^1, .., m^n). \quad (9)$$

For all our tests $n = 2048$ was used.

3.3 Estimating the 2D Growth Direction of Hair

After the distribution of facial hair has been estimated 2D texture orientations (Ω) are computed. The basic idea is to
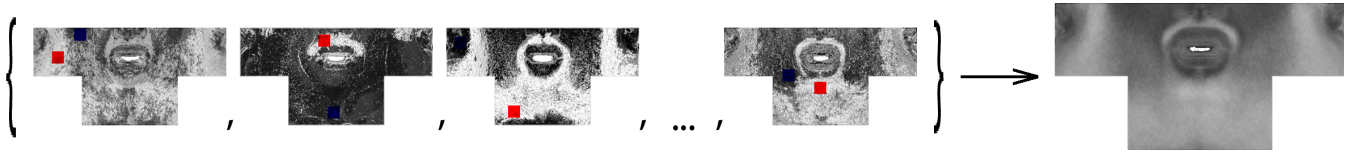
Figure 4: For improving the estimate p_{hair} for of facial hairs distribution of a target T in case of missing or incomplete information as well as for avoiding "false positive" hair texels, a "prior" is used. This prior (rightmost image) is based on a database of over 70 individuals and statistically combines relevant features present in the datasets. In each texture, the red and blue blue blocks indicate the best "learning regions" found by our iterative optimization process (see Equation 9)

recreate a 2D vector field over the facial hair region that is representing the predominant growth direction of hair.

In order to achieve this the "steerable filters" method, as proposed by Freeman and Adelson [Freeman and Adelson 1991], is used. In this approach a filter is defined by a kernel K designed to detect an x-aligned orientation. To test an arbitrary local orientation θ in pixel (i, j), K is rotated by θ and convolved with the image. Then, the "oriented energy" of the convolution — which we use to characterize the strength of orientation — is given by:

$$E_2(\theta, i, j) = [G_2^\theta(i,j)]^2 + [H_2^\theta(i,j)]^2 \qquad (10)$$

where G_2 is the second derivative of a Gaussian and H_2 is its corresponding Hilbert transform.

Dividing the interval $[-\pi/2, \pi/2]$ in equally spaced angles and testing the filter for each of these angles yields a "response curve" for each texel $t_{(i,j)}$. The predominant orientation $\Omega^{(i,j)}$ is then given by the maximum response and the inverse of the curve's variance $\omega^{(i,j)}$ as its confidence [Wei et al. 2005].

In the following p_{hair} and Ω will be summarized by a vector Γ:

$$\Gamma = \left[\begin{array}{c} p_{\text{hair}} \\ \Omega \end{array} \right]. \qquad (11)$$

3.4 A Statistical Prior for Facial Hair

In case of missing, incomplete or noisy texture estimates of Γ may be improved by taking into account statistical information about the distribution and orientation of facial hair obtained from many individuals. Assuming that a database of registered texture images $I_k, k \in \{1, .., n\}$, is given first the corresponding Γ_k distributions are computed which are then combined to a "prior" $\bar{\Gamma}$ by weighted averaging:

$$\bar{\Gamma} = \left[\begin{array}{c} \bar{p}_{\text{hair}} \\ \bar{\Omega} \end{array} \right] \qquad (12)$$

with

$$\bar{p}_{\text{hair}} = \frac{1}{\sum_k m_{\text{best}}^k} \sum_k m_{\text{best}}^k p_{\text{hair}}^k \qquad (13)$$

and

$$\bar{\Omega}^{(i,j)} = \frac{1}{\sum_k \omega_k^{(i,j)}} \sum_k \omega_k^{(i,j)} \Omega_k^{(i,j)}. \qquad (14)$$

Please note that the weights for $\bar{p}_{\text{hair}}$ — which are constant for all texels of I_k — are given by the optimal quality measure used for hair/skin classification (see section 3.2.2). Thus, results p_{hair}^k with a clear separation of skin and hair regions tend to be more effective. In contrast to $\bar{p}_{\text{hair}}$ the weights for $\bar{\Omega}^{(i,j)}$ are computed on a local basis. Here, $\omega^{(i,j)}$ locally characterizing the confidence of the 2D orientation according to section 3.3 is used implying that strongly oriented pixels are most relevant to the prior.

Once the $\bar{\Gamma}$ has been generated, it is used to improve the already estimated distributions Γ_k in a local fashion. The goal of improving Γ_k is to accentuate the separation between the hair and skin texels while keeping relevant detail of the originals and completing regions that are not well classified as either skin or hair. Intuitively, this means that regions of high uncertainty are enhanced with prior data whereas texels that have been clearly identified as skin or hair are nearly preserved. This objective is achieved by applying the prior as follows:

$$
\begin{aligned}
p_0 &= \min(p_{\text{hair}} \cdot \bar{p}_{\text{hair}}, \bar{p}_{\text{hair}}^2) \\
p_1 &= \max(p_{\text{hair}}, \sqrt{p_{\text{hair}} \cdot \bar{p}_{\text{hair}}}) \\
p_{\text{hair}}' &= \left\{ \begin{array}{ll} p_0 & 1 - p_0 > p_1 \\ p_1 & \text{otherwise} \end{array} \right.
\end{aligned}
\qquad (15)
$$

Using two different expressions p_0 and p_1 allows for accentuating the difference between skin and hair which is especially important for avoiding "false positive" hair regions (see Fig. 5).

To improve the orientation map we follow a different approach, because the goal is to improve the angle measurement. Therefore, from the estimated angle $(\Omega_k(i, j))$ and the combined one $(\bar{\Omega}(i, j))$, we select the one with the bigger confidence value.

4 Hair Synthesis

Once Γ is improved, a 3D hair geometry (a set of N filaments) is generated on the head model. As the texture images are registered, there is a correspondence between 3D model coordinates and 2D texture coordinates. This is a key element in the generation process.

4.1 Distributing Hair Roots

First we calculate the location of the filaments' roots. For this purpose a 2D sampler distributes n samples (a user defined parameter specifying the number of filaments to be synthesized), using the estimated p_{hair} as probability density function (pdf). In a subsequent step these samples are
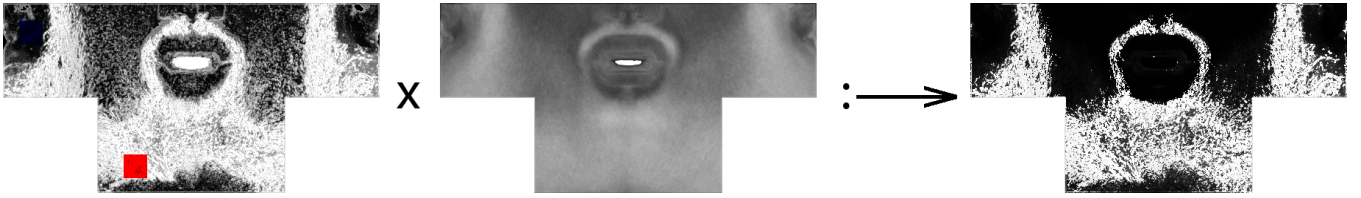
Figure 5: Improving estimates by applying the prior information (middle image) to the original p_{hair} (leftmost image). The prior allows for a much clearer separation of skin and hair and that all features of the original estimate are also present in the result of this operation (rightmost image).

then projected from 2D texture space to 3D world space. For the i-th filament the resulting 3D positions of the hair roots are denoted $\vec{P}_i$.

4.2 Generation of Filaments

The hair filaments are generated using a "particle shooting" approach: a "projectile" is "shot" from the hair root $\vec{P}_i$, using an initial orientation $\vec{O}_i$. The filament is then given by the projectile's trajectory. The vector $\vec{O}_i$ is computed as the 3D projection of the 2D orientation field Ω introduced in section 3.3. Adding a gentle pseudo gravity force $\vec{f}_g$ further improved results.

To obtain plausible results also filament-filament as well as filament-head model collisions have been taken into account. Collisions are detected using a grid based approach [Teschner et al. 2003]. The filaments are generated starting at the roots by an iterative synthesis process. In each iteration the filaments are extended according to the particle trajectories. Collisions are avoided by separating filaments that are in contact. Collisions get resolved simultaneously for all filaments within a certain predefined neighborhood.

4.2.1 Generation of Eyebrows

Eyebrow filaments are generated differently because they tend to be more aligned. For that reason no particle shooting is applied. Instead the 2D orientation field Ω is used directly as filaments growth direction. Starting at the 2D root location in texture space the filaments are tracked through Ω. The resulting trajectories are then converted to 3D world-coordinates and are terminated as they reach a predefined maximum length.

4.3 Rendering

The realistic visualization of the resultant geometry is the last step of the modeling process. In order to achieve physically-plausible results the hair shading framework proposed by Zinke and Weber [Zinke and Weber 2007] was used. It is important to note that believable results are obtained only if the rendered hair exhibits similar detail as the textures mapped on the 3D head models. This is obtained by adapting the filter width used for image reconstruction (as final part of the rendering pipeline) to the size of projected texels in image space.

5 Results

A simple example illustrating the different steps of our pipeline is given in Fig. 6.

Figures 7 and 8 show further applications of our approach: In Fig. 7 facial hair is characterized from two different sources (topmost row) and transfered to four targets (leftmost column). In the second example we aim to generate plausible beards on (nearly) completely shaved individuals (leftmost column). Taking advantage of the statistical prior in conjunction with the texture images we are able to synthesize believable results (rightmost column) even in such very challenging cases. The resulting hair distribution is very consistent with original regions which are hardly visible in the texture images. For comparison purposes also the pure prior was transfered to the models (middle column).

The most obvious limitation of our approach is that it is based on the assumption that a mapping between the 2D texture space and the 3D model space is known. That restricts our input data to registered texture images. Other limitation is that the textures in the database must be similar in order to the prior be constructed in a meaningful way.

Feature detection is the most time-consuming step of the whole process. With an Intel Core 2 Duo CPU (E8500 @ 3.16 GHz, using a single core), it takes around 45 seconds to process one model. This feature detection is required also for each of the models that are used to build the statistical prior. However, as the prior is computed only once, and remains unchanged for all subsequent analysis, it's costs (50 minutes of pre-computation our case) are usually not a limiting factor.

The other time consuming step is the geometry synthesis, whose runtime depends strongly on the number of filament to be generated. All of our examples have 11000 filaments with 10 mm maximal length each. With these parameters the hair geometry is generated in 25 seconds.

6 Conclusion and Future Work

We have presented a technique that extracts the geometric information of facial hair out of registered 2D textures and uses it for different synthesis tasks on (morphable) 3D-head models (see Figures 7 and 8). As for the existing approach a very simple heuristic was used to determine the length of a filament. An interesting topic of future work would be to infer this length directly using more sophisticated texture space analysis as well as database statistics. We did not try to extract "hair color" information from the images. Notice

Figure 6: Stages of the facial hair generation process. Starting with the 3D head model and texture images as input data (first and second images from left), the facial hair region is estimated using a probability map (middle image), the hair filaments are generated with their corresponding distributions and orientations (fourth image from left) and finally a photo-realistic image is rendered (last image)

that "hair color" is a concept that must be defined carefully on the fiber level, e.g. as the parameters of a BCSDF scattering model [Zinke and Weber 2007; Zinke et al. 2009]. Zinke et al. [Zinke et al. 2009] present a practical approach for the acquisition of hair color (the parameters of the BCSDF of an average fiber) of scalp hair out of images. This approach requires that a hair strand is wrapped around a cylinder to have a well defined hair geometry with "good" properties for solving the inverse rendering problem. Whereas this approach is not directly applicable to facial hair, the more regular geometric properties of facial hair with respect to scalp hair makes it plausible that this approach can be adapted to the problem of BCSDF estimation of facial hair fibers.

The ultimate goal of our future work is aimed to extend our techniques to the development of an approach that allows the modeling of complete hairstyles using qualitative information retrieved from images.

References

BLANZ, V., AND VETTER, T. 1999. A morphable model for the synthesis of 3d faces. In *SIGGRAPH '99: Proceedings of the 26th annual conference on Computer graphics and interactive techniques*, 187–194.

BOYKOV, Y., VEKSLER, O., AND ZABIH, R. 2001. Fast approximate energy minimization via graph cuts. *IEEE Trans. Pattern Anal. Mach. Intell. 23*, 11, 1222–1239.

FREEMAN, W. T., AND ADELSON, E. H. 1991. The design and use of steerable filters. *IEEE Transactions on Pattern Analysis and Machine Intelligence 13*, 9, 891–906.

KAKUMANU, P., MAKROGIANNIS, S., AND BOURBAKIS, N. 2007. A survey of skin-color modeling and detection methods. *Pattern Recogn. 40*, 3, 1106–1122.

KIM, T.-Y., AND NEUMANN, U. 2002. Interactive multiresolution hair modeling and editing. In *SIGGRAPH '02: Proceedings of the 29th annual conference on Computer graphics and interactive techniques*, 620–629.

LAY, T., ZINKE, A., WEBER, A., AND VETTER, T. 2009. Towards image-based beard modeling. In *SIGGRAPH ASIA '09: ACM SIGGRAPH ASIA 2009 Posters*, ACM, New York, NY, USA, 1–1.

MIHASHI, T., TEMPELAAR-LIETZ, C., AND BORSHUKOV, G. 2005. Generating realistic human hair for "the matrix reloaded". In *SIGGRAPH '05: ACM SIGGRAPH 2005 Courses*, 17.

PARIS, S., CHANG, W., KOZHUSHNYAN, O. I., JAROSZ, W., MATUSIK, W., ZWICKER, M., AND DURAND, F. 2008. Hair photobooth: geometric and photometric acquisition of real hairstyles. *ACM Trans. Graph. 27*, 3. SIGGRAPH 2008.

PAYSAN, P., KNOTHE, R., AMBERG, B., ROMDHANI, S., AND VETTER, T. 2009. A 3d face model for pose and illumination invariant face recognition. In *AVSS '09: Proceedings of the 2009 Sixth IEEE International Conference on Advanced Video and Signal Based Surveillance*, IEEE Computer Society, Washington, DC, USA, 296–301.

ROUSSET, C., AND COULON, P. 2008. Frequential and color analysis for hair mask segmentation. In *ICIP08*, 2276–2279.

TESCHNER, M., HEIDELBERGER, B., MUELLER, M., POMERANETS, D., AND GROSS, M., 2003. Optimized spatial hashing for collision detection of deformable objects.

WARD, K., BERTAILS, F., KIM, T.-Y., MARSCHNER, S. R., CANI, M.-P., AND LIN, M. 2007. A survey on hair modeling: Styling, simulation, and rendering. *IEEE Transactions on Visualization and Computer Graphics 13*, 2, 213–234.

WEI, Y., OFEK, E., QUAN, L., AND SHUM, H.-Y. 2005. Modeling hair from multiple views. *ACM Trans. Graph. 24*, 3, 816–820. SIGGRAPH 2005.

YACOOB, Y., AND DAVIS, L. S. 2006. Detection and analysis of hair. *IEEE Trans. Pattern Anal. Mach. Intell. 28*, 7, 1164–1169.

ZINKE, A., AND WEBER, A. 2007. Light scattering from filaments. *IEEE Transactions on Visualization and Computer Graphics 13*, 2, 342–356.

ZINKE, A., LAY, T., ANDRIYENKO, A., RUMP, M., WEBER, A., AND KLEIN, R. 2009. A practical approach for photometric acquisition of hair color. *ACM Trans. Graph. 28*, 5. SIGGRAPH ASIA 2009.

Figure 7: Beard transfer. Two different sources (topmost row) are used to synthesize beards on four different targets (leftmost column).
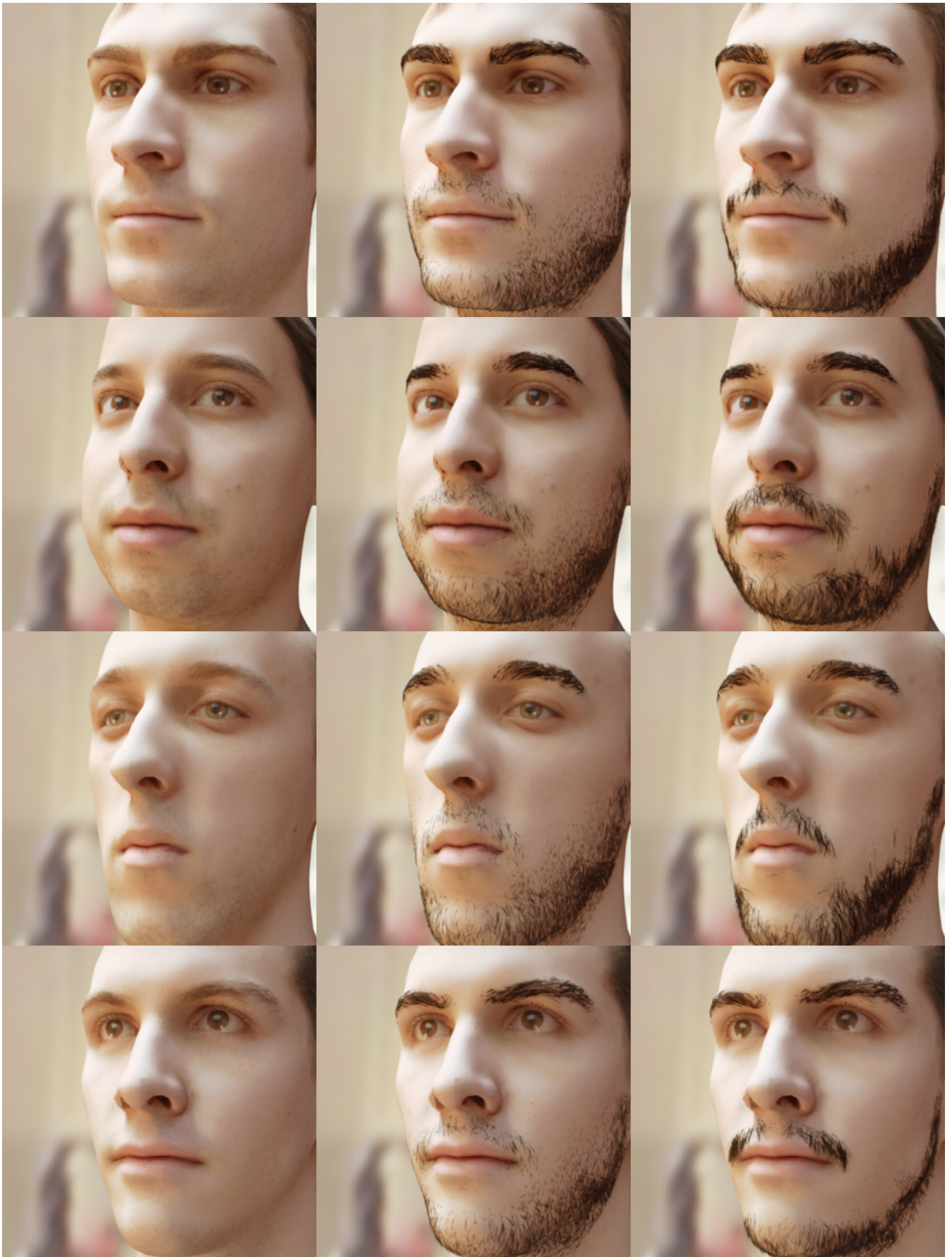
Figure 8: Applying our method to shaved individuals (first column). Results obtained by using exclusively information from our statistical prior (middle row) and the final results also taking into account the specific characteristics of individuals according to the full pipeline (rightmost row).